JMEPEG (2017) 26:4177–4187
DOI: 10.1007/s11665-017-2857-6
©ASM International
1059-9495/$19.00
CrossMark

The Effect of Wetting Gravity Regime on Shear Strength of SAC and Sn-Pb Solder Lap Joints

Mrunali Sona and K. Narayan Prabhu

(Submitted January 28, 2017; in revised form July 2, 2017; published online August 16, 2017)

The failure of solder joints due to imposed stresses in an electronic assembly is governed by shear bond strength. In the present study, the effect of wetting gravity regime on single-lap shear strength of Sn-0.3Ag-0.7Cu and Sn-2.5Ag-0.5Cu solder alloys reflowed between bare copper substrates as well as Ni-coated Cu substrates was investigated. Samples were reflowed for 10 s, T_{gz} (time corresponding to the end of gravity regime) and 100 s individually and tested for single-lap shear strength. The single-lap shear test was also carried out on eutectic Sn-Pb/Cu- and Sn-Pb/Ni-coated Cu specimens to compare the shear strength values obtained with those of lead-free alloys. The eutectic Sn-Pb showed significantly higher ultimate shear strength on bare Cu substrates when compared to Sn-Ag-Cu alloys. However, SAC alloys reflowed on nickel-coated copper substrate exhibited higher shear strength when compared to eutectic Sn-Pb/Ni-coated Cu specimens. All the substrate/solder/substrate lap joint specimens that were reflowed for the time corresponding to the end of gravity regime exhibited maximum ultimate shear strength.

Keywords lead-free solders, single-lap shear test, ultimate shear strength, wetting gravity regime

1. Introduction

The electronics industry has transformed from lead based to lead-free electronics to comply with government legislations restricting the usage of lead. Soldering plays a crucial role in electronic, automobile and aircraft industries where components need to be joined together with sufficient mechanical integrity (Ref 1, 2). Sn-Ag-Cu is a most widely accepted lead-free alloy for the replacement of conventional Pb-Sn solder. Sn-Ag-Cu alloys have moderately low melting temperature, better solderability, and superior mechanical properties when compared to any other tin-rich alloys (Ref 3). However, reliability issues of the lead-free solder joints remain as a great concern. Therefore, solder joint strength appears to be a key factor to be assessed to have a reliable solder joint (Ref 4, 5). Mechanical properties of the solder joint are often influenced by the microstructure of the solder joint. Evolution of microstructure is in turn influenced by various parameters such as solder composition, substrate used, reflow time, reflow temperature, cooling rate, and thermo mechanical processing. Eutectic or near-eutectic alloys generally form a rigid joint due to their faster solidification rate as they do not pass through a weak pasty stage (Ref 2). Hence, they are preferred in most of the electronic assemblies when compared to a hypo or hyper eutectic alloy. Cu, Ni and Au are the common base metallic substrates used in electronic products. As soon as the molten solder touches the base metal surface, an intermetallic compound (IMC) layer forms instantly at the solder/substrate interface. These IMCs are inherently brittle and have greater propensity to produce structural defects. Therefore, a thick IMC layer at the solder/substrate interface may reduce the reliability of the solder joint but a thin consistent and continuous IMC layer is required for strong bonding (Ref 6). Ni has good wetting characteristics with Sn and also the stable phases, which it forms with Sn in the Ni-Sn binary system, has a slower growth rate when compared with the Cu intermetallic compounds. Therefore, the surfaces of the Cu substrates are generally coated with a Ni layer to reduce the direct interaction between solder and Cu substrate (Ref 7).

Stress load is one of the major reasons for the failure of electronic components and it arises when the device is mishandled or dropped. Therefore, stress load analysis is vital to ensure that the solder joints are capable of holding various stress loads during service conditions. Pang et al. (Ref 8) investigated the effect of test temperature and strain rate on shear strength of Sn-3.8Ag-0.7Cu/Cu single-lap solder joint. Samples were reflowed at 235, 240, and 250 °C. The test was carried out at three test temperatures (25, 75, and 125 °C) and under three strain rates 2.6×10^{-2}, 2.6×10^{-3} and 2.6×10^{-4} s^{-1}. The mechanical strength of 95.5Sn-3.8Ag-0.7Cu solder joint decreased with increase in test temperature and increased with increase in strain rate. Affendy et al. (Ref 5) investigated the effect cross head speed on joint shear strength of Sn-9Zn/Cu single-lap joints. The samples were prepared by reflowing Sn-9Zn/Cu system at 220 °C for 30 s followed by air cooling. The measurement was taken in a range of crosshead speed values from 0.5 to 3.0 mm/min, with increments of 0.5. Sn-9Zn/Cu lap joints showed increasing solder strength with increasing crosshead speeds. Jeong et al. (Ref 9) investigated the effect of cooling rate on fracture mode of Sn-3.5Ag/Cu, Sn-3.0Ag-0.7Cu/Cu, Sn-3.0Ag1.5Cu/Cu, Sn-3.7Ag-0.9Cu/Cu, and Sn-6.0Ag-0.5Cu/Cu lap joints. The solder alloy was reflowed at 250 °C for 60 s on Cu substrate and three different cooling media were used to control the cooling rate namely fast cooling (water quenching), medium cooling (cooling on an aluminum block), and slow cooling (furnace cooling). An inverse relationship between thickness of the interfacial IMC layer

Mrunali Sona and **K. Narayan Prabhu**, Department of Metallurgical and Materials Engineering, National Institute of Technology Karnataka, Surathkal, Mangalore 575 025, India. Contact e-mail: prabhukn_2002@yahoo.co.in.

and the shear strength was observed. Lee et al. (Ref 7) have studied the effect of aging on shear strength of Sn-Ag-*X*Ni/Cu single-lap solder joints. Sn-Ag-*X*Ni/Cu single-lap solder joints were reflowed at 260 °C for 60 s and then air-cooled. The tests were carried out at ambient conditions under a strain rate of 1×10^{-2} s^{-1}. An increase in the shear strength of as-reflowed lap joint specimens was observed with increasing Ni addition. However, a decrease in the shear strength was observed in thermally aged lap joint specimens regardless of their Ni content. Coarsening of solder microstructure was the prime reason behind the reduction in shear strength. Wei et al. (Ref 6) observed similar results while studying the effect of aging on shear strength of AuSn20/Ni-metalized Cu single-lap joints. Rani et al. (Ref 2) have investigated shear strength of Sn-37Pb/Cu, Sn-58Bi/Cu, Sn-0.7Cu/Cu, Sn-3.5Ag/Cu, Sn-9Zn/Cu and Sn-57Bi-1.3Zn/Cu single-lap joints at a strain rate of 5.5×10^{-4} s^{-1}. Sn-9Zn/Cu showed approximately 50% increase in shear strength when compared to Sn-37Pb/Cu joints. All the lead-free lap joint systems except Sn-0.7Cu/Cu showed better shear strength compared to eutectic lead-tin system.

The present study is focused on the effect of wetting gravity regime on lap shear strength of Sn-0.3Ag-0.7Cu/Cu, Sn-0.3Ag-0.7Cu/Ni-plated Cu, Sn-2.5Ag-0.5Cu/Cu and Sn-2.5Ag-0.5Cu/Ni-plated Cu lap joints. We have carried out similar experiments on the effect of reflow time on joint strength of various solder/substrate systems (Ref 10, 11), but in all the previous papers ball shear test was performed to assess the joint strength. The present investigation is an extension of the previous work. In the present work, lap shear test was performed as it represents the real condition of joint failure when compared to the ball shear test. The single-lap shear strength of lead-free solder alloys reflowed on bare and Ni-coated copper substrates was also compared with that of eutectic Sn-Pb/Cu- and Sn-Pb/Ni-coated Cu lap joints.

2. Experimental Procedure

Lap shear technique is one of the most widely used techniques for evaluating the shear, creep, and thermal fatigue behavior of solder joints. Here, the solder is placed between two substrate blocks, which are pulled in opposite directions to provide shear loading. In the present investigation, shear test is designed according to the "Test method for shear tensile fatigue of spot-weld joints" (GB/T151n-94). Figure 1 represents a schematic of the lap shear geometry. Smooth-surfaced Cu sheet was cut into rectangular plates of dimensions 50 mm × 6 mm × 1 mm. An equal number of Cu plates were metalized with Ni layer of thickness about 15 µm by electroplating method. The surface profiles of both bare and Ni-coated Cu plates were measured using Form Talysurf 50 surface profiler. The R_a value of bare and Ni-coated Cu plate was in the range of 0.03 ± 0.008 and 0.04 ± 0.007 µm, respectively. The commercial Sn-0.3Ag-0.7Cu (Alpha Electronics Manufacturers, UK) and Sn-2.5Ag-0.5Cu solder alloy (Antex Electronics Ltd.) were used in the present study. Solder alloys were cut into small pieces of dimensions 5 mm × 5 mm × 0.5 mm, and one such piece was placed between two isometallic plates. To confirm proper alignment of the solder joint, a uniaxial fixture was used for sample preparation. After the application of a drop of inorganic acid flux, the substrate/solder/substrate system was placed inside a tubular furnace (Fig. 2) which is maintained at 270 °C. Similarly, lap joint specimens of eutectic Sn-Pb solder alloy were prepared by placing eutectic Sn-Pb between two isometallic plates and keeping inside a tubular furnace which is maintained at 240 °C. Samples were reflowed for 10 s, T_{gz} (time corresponding to the end of gravity regime) and 100 s individually. Reflow time was counted as the solder started spreading. At the end of reflow time, the substrate/solder/substrate system was quenched in water kept beneath the tubular furnace. Samples were prepared in air atmosphere as in most of the industries samples are prepared in the same atmosphere particularly in the case of hand soldering. The single-lap solder joints were tested at room temperature under a strain rate of 0.2×10^{-3} s^{-1} in a pull test carried out using INSTRON 5967 tensile tester. Stress–strain graphs were recorded during the test. Three trials were carried out for each reflow time. The maximum stress value which is also known as ultimate shear strength (USS) was noted in all the lap joint tests. After the test, failure mode was assessed by examining the fractured surface under the scanning electron microscope (SEM, JEOL JSM 6380LA).

3. Results and Discussion

3.1 Single-Lap Shear Test of SAC Solder/Cu Systems

Wetting plays a key role in the formation of a metallurgical bond at the solder–substrate interface, describing the level of contact between a fluid and solid (Ref 12). The wetting or spreading behavior of a spherical solder ball involves continuous change in the contact angle with time. The spreading behavior of the solder alloy was classified into capillary, gravity

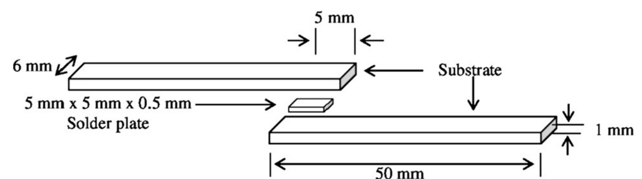

Fig. 1 Schematic of the lap shear geometry

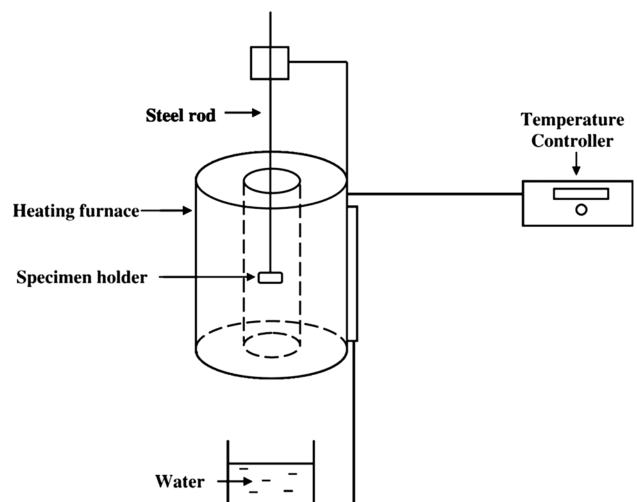

Fig. 2 Schematic of quench cooling set up

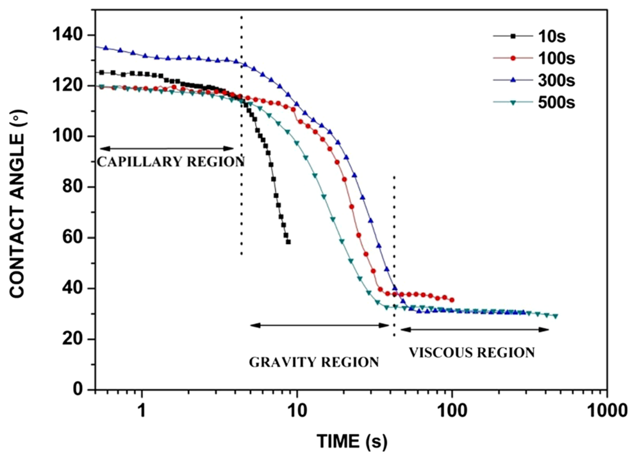

Fig. 3 Relaxation curves for Sn-2.5Ag-0.5Cu on bare Cu substrate

Fig. 4 Side view of Cu/solder/Cu lap solder joint

(diffusion), and viscous zones. Figure 3 represents typical relaxation curves for the spreading of Sn-2.5Ag-0.5Cu solder alloy on Cu substrate. The time corresponding to the end of gravity zone is termed as T_{gz}. Formation of IMCs take place at the gravity zone. The significance of T_{gz} is discussed in our previous work (Ref 10, 11). A reflow time of T_{gz}, 10 and 100 s was used in the present study. Single-lap joint tests were performed on Sn-0.3Ag-0.7Cu/Cu and Sn-2.5Ag-0.5Cu/Cu lap joints. The photograph of single-lap joints is shown in Fig. 4. The typical stress–strain graphs obtained during the lap joint test on Sn-0.3Ag-0.7Cu/Cu and Sn-2.5Ag-0.5Cu/Cu lap joints are shown in Fig. 5 and 6, respectively. Three trials were carried out for each reflow time. The maximum stress value which is also known as ultimate shear strength (USS) was noted in all the lap joint tests. The USS values obtained from the experiments are tabulated in Table 1. The area under the stress–strain curve was also calculated (toughness) and given in Table 1. The Sn-2.5Ag-0.5Cu/Cu lap joints reflowed for 40 s showed approximately 24% increase in the USS value compared to that of Sn-0.3Ag-0.7Cu/Cu lap joints reflowed for T_{gz}. At a reflow time of 10 s and 100 s, both the systems showed comparable shear strength values. Samples reflowed for T_{gz} showed maximum strength in both the systems supporting the results of our previous work (Ref 10). The toughness value was also found to be maximum at T_{gz}.

Fractographical study of sheared surfaces was carried out under SEM. Figure 7 shows the macroscopic image of fractured surface of Sn-2.5Ag-0.5Cu/Cu system reflowed for

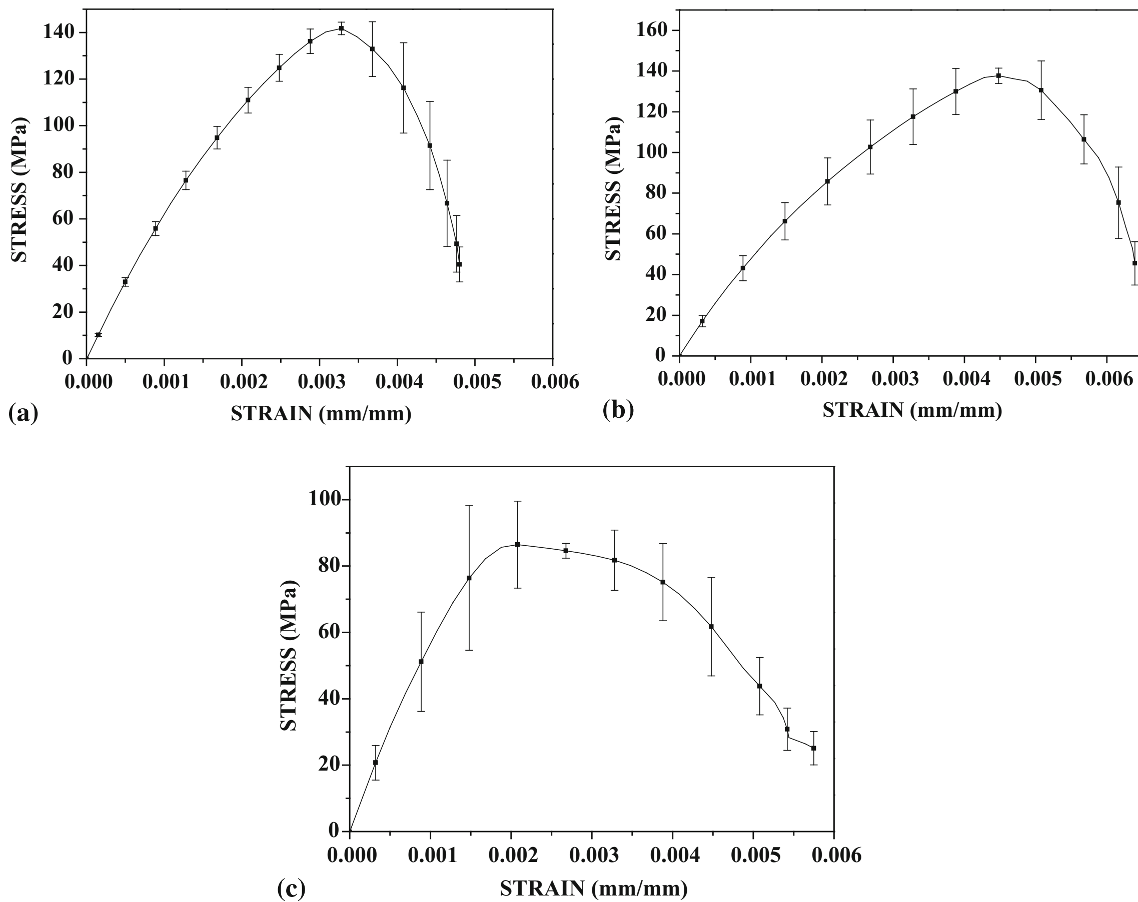

Fig. 5 Stress vs. strain plots for single-lap Sn-0.3Ag-0.7Cu/Cu joint reflowed for (a) 10 s (b) 40 s and (c) 100 s

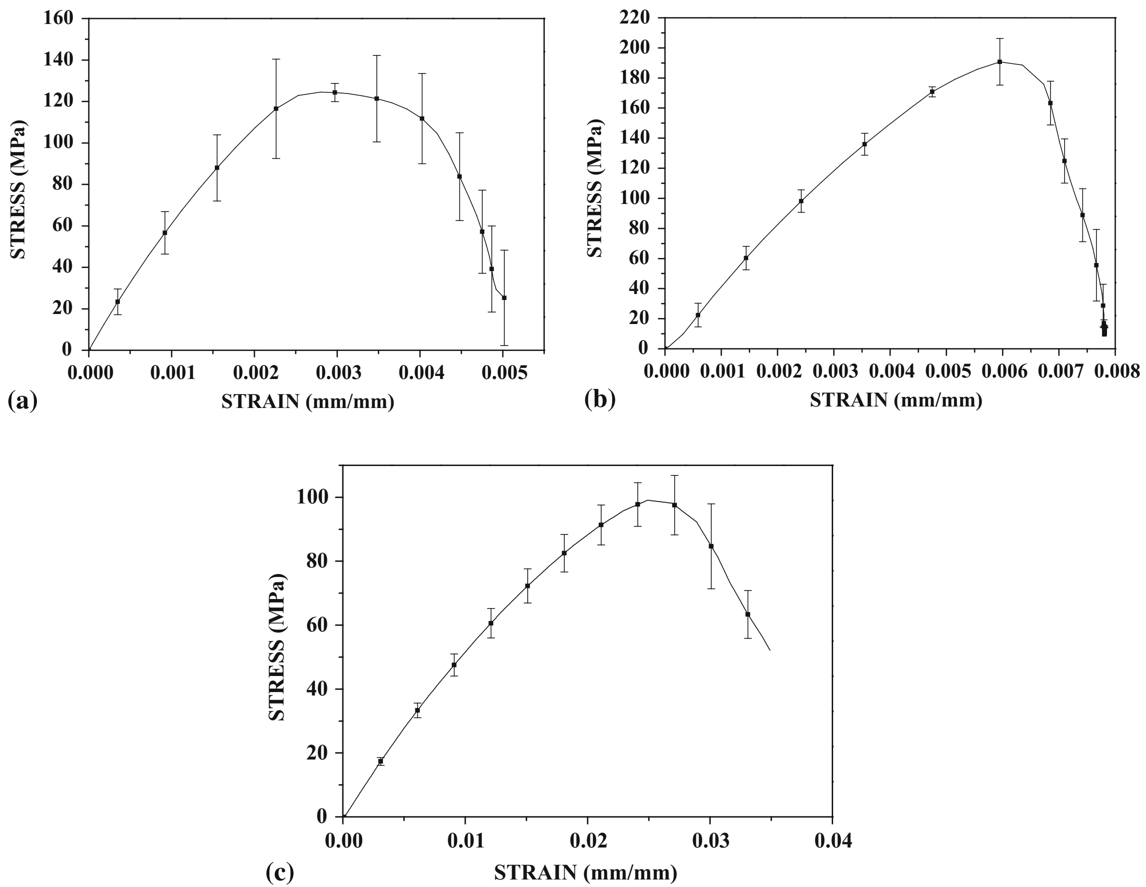

Fig. 6 Stress vs. strain plots for single-lap Sn-2.5Ag-0.5Cu/Cu joint reflowed for (a) 10 s (b) 40 s and (c) 100 s

Table 1 Lap shear strength and toughness of Sn-0.3Ag-0.7Cu/Cu and Sn-2.5Ag-0.5Cu/Cu systems

Sn-0.3Ag-0.7Cu/Cu			Sn-2.5Ag-0.5Cu/Cu		
Reflow time, s	Ultimate shear strength, MPa	Toughness, MJ/m^3	Reflow time, s	Ultimate shear strength, MPa	Toughness, MJ/m^3
10	140.38 ± 1.90	0.45 ± 0.02	10	142.45 ± 4.82	0.45 ± 0.02
40	145.79 ± 3.52	0.56 ± 0.05	40	180.74 ± 5.51	0.83 ± 0.13
100	93.54 ± 6.53	0.33 ± 0.02	100	100.67 ± 5.46	0.23 ± 0.02

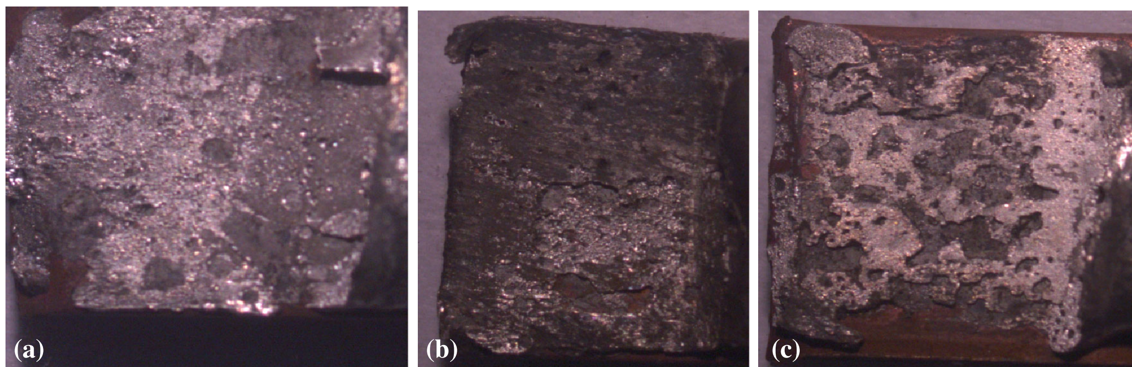

Fig. 7 Macroscopic image of fractured Sn-2.5Ag-0.5Cu/Cu system reflowed for (a) 10, (b) 40 s and (c) 100 s

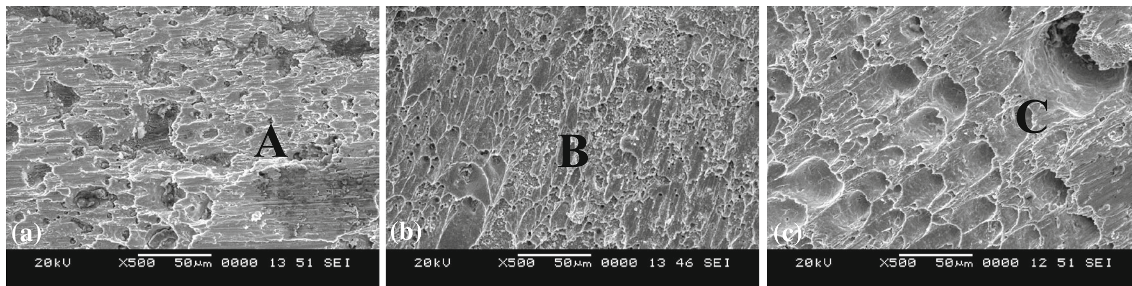

Fig. 8 SEM micrographs of fractured surfaces of single-lap Sn-0.3Ag-0.7Cu/Cu joint reflowed at (a) 10 s (b) 40 s and (c) 100 s

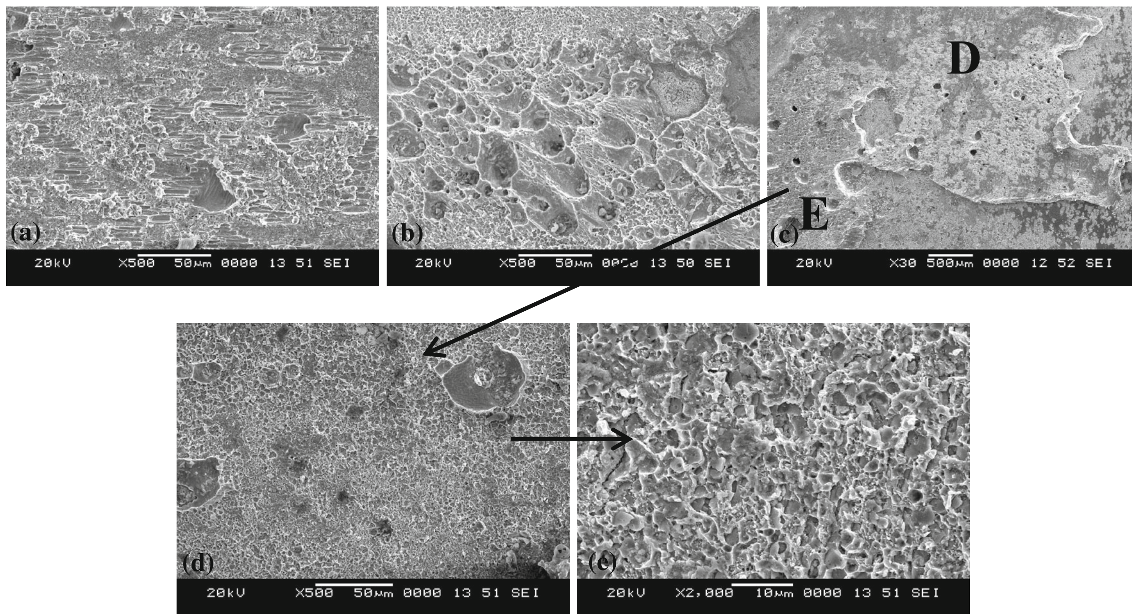

Fig. 9 SEM micrographs of fractured surfaces of single-lap Sn-2.5Ag-0.5Cu/Cu joint reflowed at (a) 10 s (b) 40 s (c) 100 s and (d), (e) show the enlarged view of the parts indicated by the arrow mark

Table 2 EDS analysis results of marked regions in Fig. 8 and 9 for Sn-0.3Ag-0.7Cu and Sn-2.5Ag-0.5Cu solder on Cu substrate

Marks	Cu K, at.%	Ag L, at.%	Sn L, at.%	Phase
A	0.38	…	99.62	Sn
B	0.24	…	99.76	Sn
C	0.45	…	99.55	Sn
D	0.65	…	99.35	Sn
E	52.53	0.35	47.12	Cu_6Sn_5

10, 40 and 100 s. There was no complete detachment of solder, and the substrate was observed in any of the systems. In general, solder joint failure takes place in three different ways. (1) Failure at the bulk solder, (2) fracture starts across the solder bulk region then diverts its path toward the solder/Cu interface and (3) total failure across the solder/Cu interface. Affendy et al. (Ref 8) observed a failure in the bulk solder at lower crosshead speed (0.5-1 mm/min). At medium crosshead speed (1.5-2 mm/min), second type of fracture was observed. At higher crosshead speeds (2.5-3 mm/min), total failure across the solder/Cu interface was observed. In the present study, single-lap solder joints were tested at ambient temperature

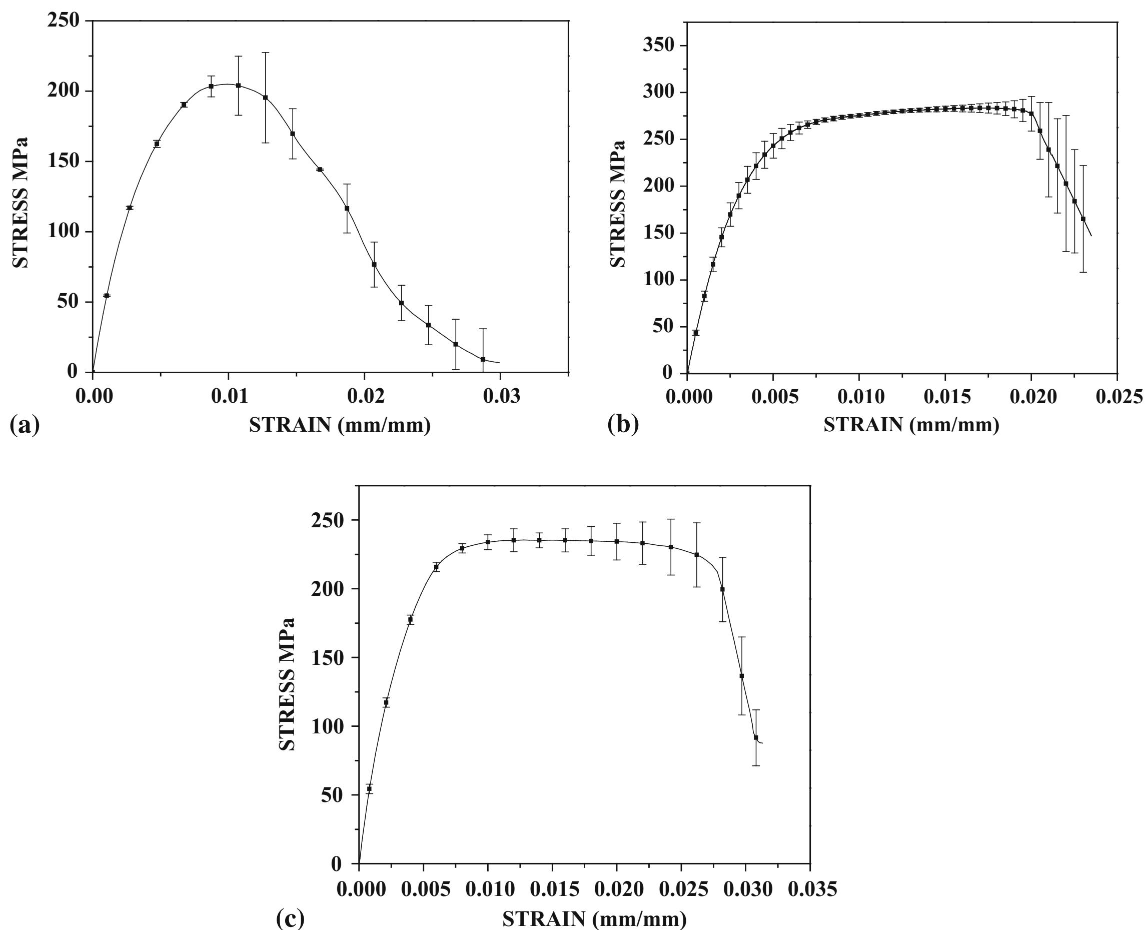

Fig. 10 Stress vs. strain plots for single-lap Sn-0.3Ag-0.7Cu/Ni-coated Cu joint reflowed for (a) 10 s (b) 70 s and (c) 100 s

under a strain rate of 0.2×10^{-3} s^{-1}. Figure 8 and 9 show the SEM images of fractured surfaces of Sn-0.3Ag-0.7Cu/Cu and Sn-2.5Ag-0.5Cu/Cu samples, respectively. All the Sn-0.3Ag-0.7Cu/Cu specimens were found to be fractured within the solder matrix, suggesting that the solder matrix is fragile than the IMC layer at the solder/Cu substrate interface. Besides, elongated dimple-like structures were observed on the Sn-0.3Ag-0.7Cu/Cu-fractured surfaces. Hence, it is apparent that Sn-0.3Ag-0.7Cu/Cu failed with a ductile fracture mode, irrespective of their reflow time conditions. Sn-2.5Ag-0.5Cu/Cu specimens reflowed for 10 s and T_{gz} (time corresponding to the end of gravity regime) fractured within the solder matrix. However, the samples reflowed for 100 s showed a fracture initiation at the bulk region followed by a diversion in fracture path toward the solder/Cu interface. Solder bulk region suffered a ductile failure, whereas fracture at the solder/IMC layer exhibited brittle failure. Figure 9(e) shows the partial debonding failure that occurred at the interface between the solder matrix and the Cu_6Sn_5 IMC layer. The faceted appearance of the fracture surfaces is due to the cleavage fracture of the Cu_6Sn_5 IMC layer. Under ball shear test, all the solder/substrate systems had showed ductile failure in the bulk matrix regardless of reflow time (Ref 10, 11). Table 2 gives the EDS analysis report of marked regions in Fig. 8 and 9.

3.2 Single-Lap Shear Test of SAC Solder/Ni-Coated Cu Systems

The typical stress–strain graphs obtained during the lap joint test on Sn-0.3Ag-0.7Cu/Ni-coated Cu and Sn-2.5Ag-0.5Cu/Ni-coated Cu lap joints are shown in Fig. 10 and 11, respectively. The USS values obtained from the experiments are tabulated in Table 3. At lower reflow time 10 s and T_{gz}, the ultimate shear strength of Sn-0.3Ag-0.7Cu/Ni-coated Cu and Sn-2.5Ag-0.5Cu/Ni-coated Cu lap joints was comparable. At a reflow time of 100 s, Sn-2.5Ag-0.5Cu/Ni-coated Cu lap joints showed about 13% increase in the USS value when compared with Sn-0.3Ag-0.7Cu/Ni-coated Cu lap joints. However, the USS values were found to be maximum for samples reflowed for time corresponding to the end of gravity zone. Both the solder alloys showed significantly higher ultimate shear strength when

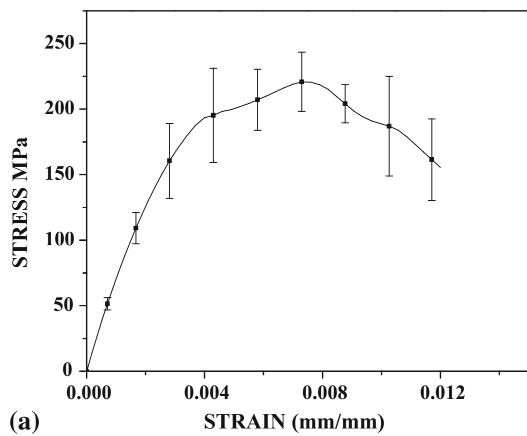

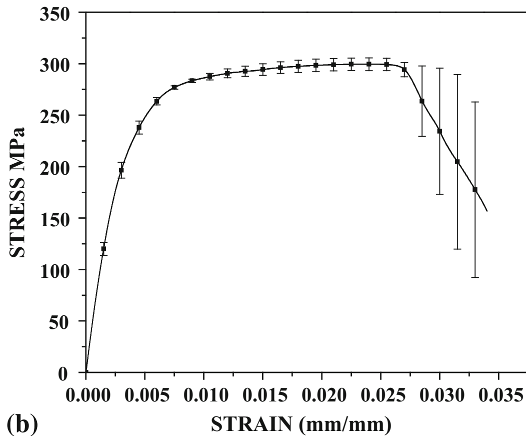

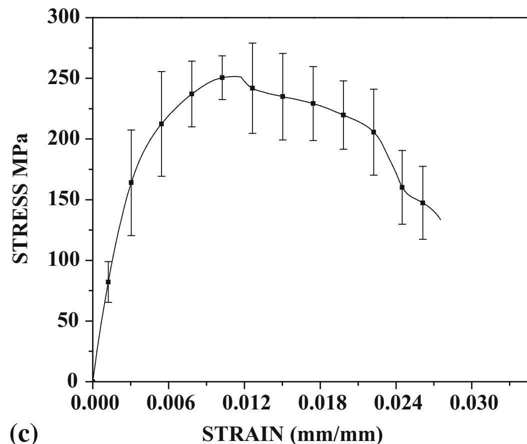

Fig. 11 Stress vs. strain plots for single-lap Sn-2.5Ag-0.5Cu/Ni-coated Cu joint reflowed for (a) 10 s (b) 80 s and (c) 100 s

reflowed on Ni-coated Cu substrates rather than bare Cu substrate. This is due to lower reaction rate of Ni with Sn than that of Cu with Sn. Hence, Ni acts as a diffusion barrier layer for Cu/Sn-based solders in electronics. In addition, the use of Ni improves solidification microstructure, thereby decreasing the tendency of crack formation at the interfacial IMCs during service (Ref 10).

Single-lap solder joint specimen of Sn-0.3Ag-0.7Cu/Ni-coated Cu substrate and Sn-2.5Ag-0.5Cu/Ni-coated Cu substrate reflowed for 10 s and T_{gz} failed at the bulk solder, whereas specimens reflowed for 100 s showed partial debonding failure at the solder matrix/$(CuNi)_6Sn_5$ IMC layer interface. The nodular tips of $(CuNi)_6Sn_5$ IMC layer were protruded into fractured surfaces. Under stress load condition, the $(CuNi)_6Sn_5$ nodular tips produce a large shear strain localization effect. Consequently, the IMC interface becomes the favored site for crack formation and propagation. Figure 12 and 13 show the partial debonding failure at the solder matrix/$(CuNi)_6Sn_5$ IMC layer interface. In Fig. 12(d) and 13(d), faceted structure on the fracture surface can be observed. Cleavage fracture of the $(CuNi)_6Sn_5$ layer is the reason for the faceted appearance. When the cleavage planes in neighboring $(CuNi)_6Sn_5$ grains are relatively parallel, the fracture can easily propagate through the IMC layer or along the $(CuNi)_6Sn_5$ layer/solder matrix interface (Ref 7). Under ball shear test, all the solder/Ni-coated Cu substrate systems had showed ductile failure in the bulk matrix up to a reflow time of 500 s (Ref 10, 11). Table 4 gives the EDS analysis report of marked regions in Fig. 12 and 13.

Lap joint tests of Sn-37Pb/Cu and Sn-37Pb/Ni-coated Cu single-lap solder joints were carried out to compare the shear strength values obtained with lead-free solder alloys. Three reflow times chosen were 10, 100 and T_{gz}. T_{gz} for Sn-Pb/Cu- and Sn-Pb/Ni-coated Cu systems was found to be 7 and 14 s, respectively, from the wetting characterization test. Figure 14 shows the stress versus strain graphs for Sn-37Pb solidified between Cu plates for 7, 10 and 100 s, respectively. Table 5 gives the USS values obtained for the test. Samples reflowed for 7 s gave maximum strength among Sn-Pb solidified between bare Cu substrates for various reflow times. Figure 15 shows the stress versus strain graphs for Sn-Pb solidified between Ni-coated Cu plates for 10, 14 and 100 s, respectively. Samples reflowed for 14 s gave the maximum strength. At T_{gz}, both Sn-Pb/Cu and Sn-Pb/Ni/Cu showed comparable strength. It is well established from the literature that Sn-Pb lap joints exhibits boundary layer fracture where the fracture takes place within the solder material, close to the interface instead of occurring exactly at the interface (Ref 13-15). During early stage of the test, elastic deformation of the specimen takes place. An interphase debonding occurs within the solder with increase in load, leading to crack initiation at the region of shear

Table 3 Lap shear strength and toughness of Sn-0.3Ag-0.7Cu/Ni/Cu and Sn-2.5Ag-0.5Cu/Ni/Cu systems

Sn-0.3Ag-0.7Cu/Ni/Cu			Sn-2.5Ag-0.5Cu/Ni/Cu		
Reflow time, s	Ultimate shear strength, MPa	Toughness, MJ/m^3	Reflow time, s	Ultimate shear strength, MPa	Toughness, MJ/m^3
10	241.89 ± 6.25	3.39 ± 0.16	10	250.53 ± 5.62	3.13 ± 0.39
70	280.09 ± 4.37	8.74 ± 0.39	80	291.56 ± 6.31	9.45 ± 0.79
100	245.57 ± 3.38	6.44 ± 0.5	100	278.67 ± 4.52	5.51 ± 0.54

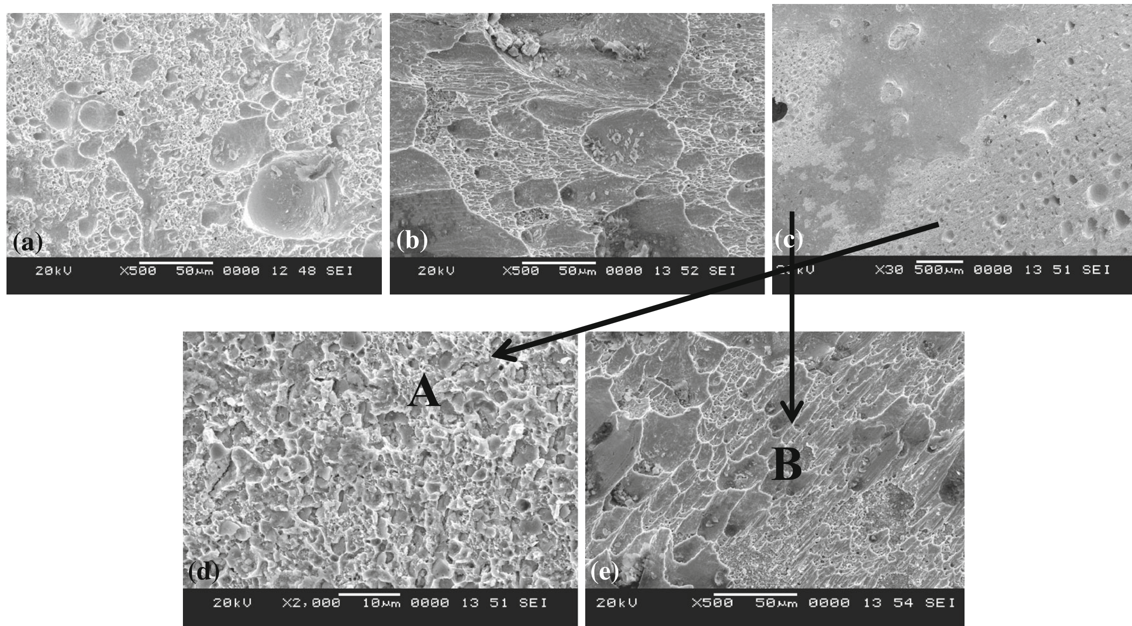

Fig. 12 SEM micrographs of fractured surfaces of single-lap Sn-0.3Ag-0.7Cu/Ni/Cu joint reflowed at (a) 10 s (b) 70 s (c) 100 s and (d), (e) show the enlarged view of the parts indicated by the arrow mark

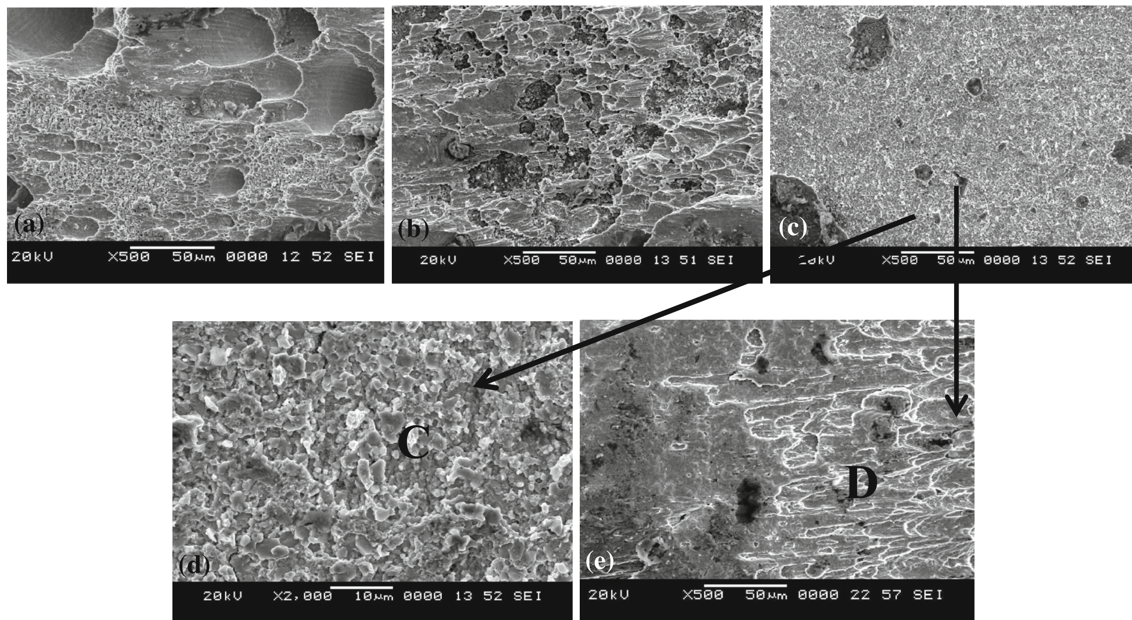

Fig. 13 SEM micrographs of fractured surfaces of single-lap Sn-2.5Ag-0.5Cu/Ni/Cu joint reflowed at (a) 10 s (b) 80 s (c) 100 s and (d), (e) show the enlarged view of the parts indicated by the arrow mark

Table 4 EDS analysis results of marked regions in Fig. 12 and 13 for Sn-0.3Ag-0.7Cu and Sn-2.5Ag-0.5Cu on Ni-coated Cu substrate

Marks	Cu K, at.%	Ag L, at.%	Sn L, at.%	Ni K, at.%	Phase
A	31.77	0.34	48.62	19.27	$(CuNi)_6Sn_5$
B	0.25	…	99.75	…	Sn
C	33.42	0.27	45.57	20.74	$(CuNi)_6Sn_5$
D	0.85	…	99.15	…	Sn

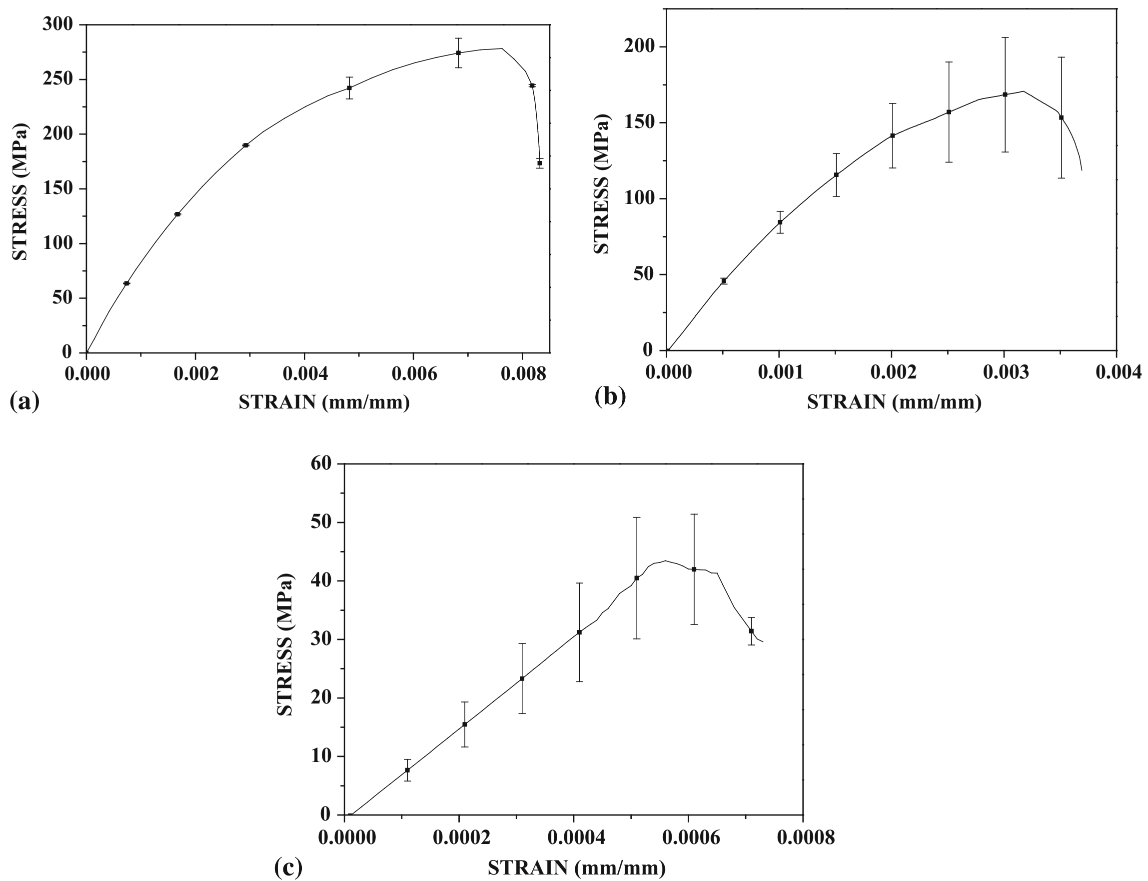

Fig. 14 Stress vs. strain plots for single-lap Sn-Pb/Cu joint reflowed for (a) 7 s (b) 10 s and (c) 100 s

Table 5 Lap shear strength and toughness of Sn-Pb/Cu and Sn-Pb/Ni/Cu systems

Sn-Pb/Cu			Sn-Pb/Ni/Cu		
Reflow time, s	Ultimate shear strength, MPa	Toughness, MJ/m^3	Reflow time, s	Ultimate shear strength, MPa	Toughness, MJ/m^3
7	275.73 ± 10.38	1.65 ± 0.16	10	182.25 ± 6.54	1.02 ± 0.28
10	170.63 ± 11.63	0.43 ± 0.06	14	260.65 ± 5.91	3.57 ± 1.88
100	50.85 ± 3.03	0.03 ± 0.02	100	238.24 ± 4.45	2.31 ± 0.44

stress concentration followed by crack propagation toward the center of the solder. A narrow zone of debonded grains forms in front of the crack. Microcracks and microvoids coalesce within the solder material with further increase in load. Thus, formed macrocrack extends fully across the specimen resulting in ductile shear fracture of the specimen (Ref 13).

This study confirms that Sn-0.3Ag-0.7Cu and Sn-2.5Ag-0.5Cu can be used as substitute alloy for eutectic Sn-Pb on Ni-coated Cu substrate. SAC and Sn-Pb alloys showed maximum joint strength at T_{gz} irrespective of the substrate material used. This investigation clearly brings out the effect of gravity wetting regime on shear strength of the solder lap joints.

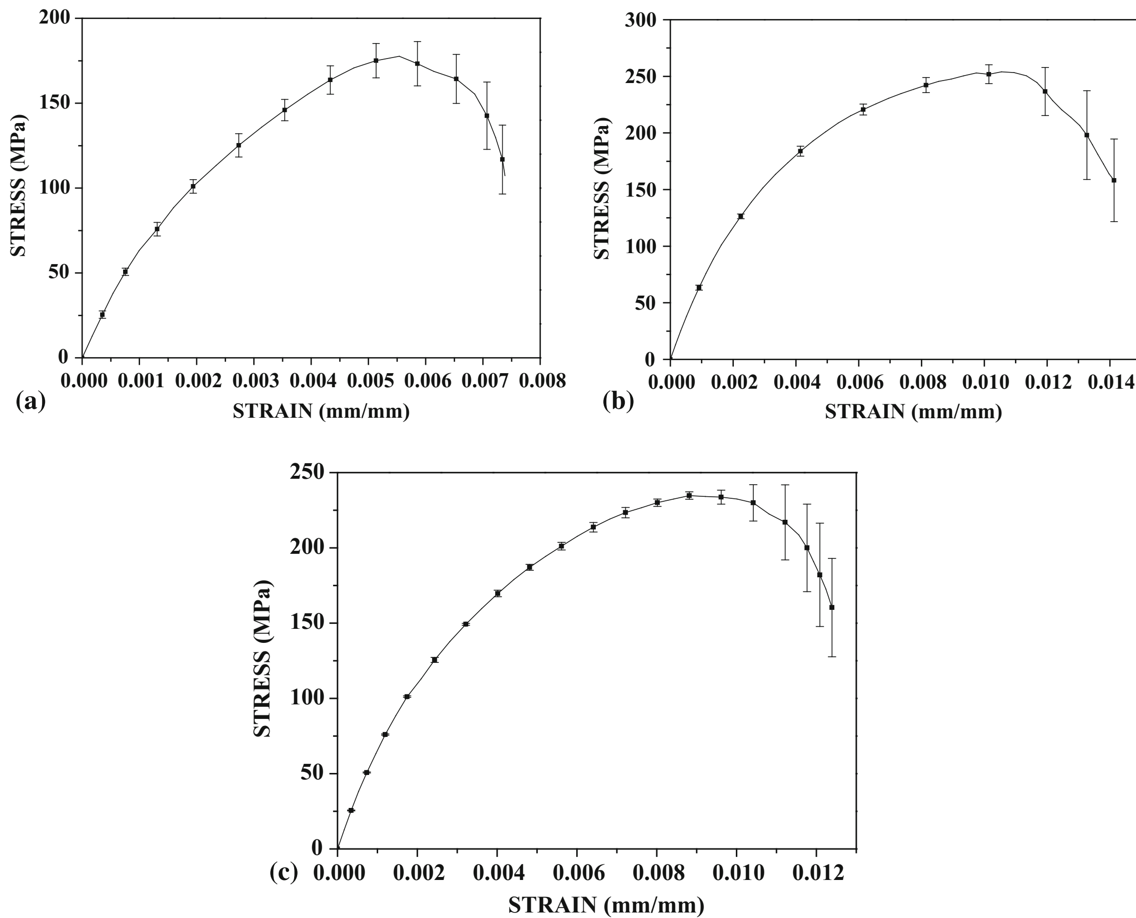

Fig. 15 Stress vs. strain plots for single-lap Sn-Pb/Ni/Cu joint reflowed for (a) 10 s (b) 14 s and (c) 100 s

4. Conclusion

Based on the study of the effect of reflow time on lap joint strength of Sn-0.3Ag-0.7Cu/Cu, Sn-0.3Ag-0.7Cu/Ni-coated Cu, Sn-2.5Ag-0.5Cu/Cu and Sn-2.5Ag-0.5Cu/Ni-coated Cu systems, the following conclusions were drawn.

1. Single-lap solder joints reflowed till the end of gravity zone time (T_{gz}) showed maximum joint strength.
2. Sn-0.3Ag-0.7Cu/Cu showed a ductile failure at the bulk matrix irrespective of reflow time. Sn-2.5Ag-0.5Cu/Cu specimens reflowed for 10 s and T_{gz} (time corresponding to the end of gravity regime) fractured within the solder matrix, whereas in samples reflowed for 100 s, fracture started at the bulk region followed by diversion in the fracture path to the solder/Cu interface. Fracture at the solder/IMC interface exhibited brittle failure.
3. Sn-0.3Ag-0.7Cu and Sn-2.5Ag-0.5Cu solder alloys reflowed for 10 s and T_{gz} on Ni-coated Cu substrate failed at the bulk solder, whereas specimens reflowed for 100 s showed partial debonding failure at the interface between the solder matrix and the $(CuNi)_6Sn_5$ IMC layer.
4. SAC alloys reflowed on Ni-coated Cu substrates showed higher shear strength when compared to that of same alloys reflowed on bare Cu substrates. This clearly shows that Ni acts as a diffusion barrier and hence improves the joint strength. A reflow time of 40 s is optimum for Sn-0.3Ag-0.7Cu and Sn-2.5Ag-0.5Cu alloy on Cu substrate, and 70-80 s is optimum for Sn-0.3Ag-0.7Cu and Sn-2.5Ag-0.5Cu alloy on Ni-coated Cu substrate to have a maximum joint strength. It was observed that T_{gz} for solder alloys on Ni-coated copper substrate is almost twice the value on bare copper substrate.
5. Single-lap shear strength of eutectic Sn-Pb on bare and Ni-coated Cu substrates were determined to compare the results obtained with lead-free solder alloys. The eutectic Sn-Pb/Cu showed approximately 53 and 89% increase in ultimate shear strength when compared to Sn-2.5Ag-0.5Cu/Cu joints and Sn-0.3Ag-0.7Cu/Cu joints, respectively. Sn-0.3Ag-0.7Cu/Ni-coated Cu and Sn-2.5Ag-0.5Cu/Cu/Ni-coated Cu showed 10% increase in ultimate shear strength when compared to and Sn-Pb/Ni-coated Cu specimens. A reflow time of 7 and 14 s is optimum for eutectic Sn-Pb on bare and Ni-coated Cu substrate, respectively.
6. The toughness of solder/substrate system was found to be maximum at T_{gz}. SAC/Ni/Cu systems showed higher toughness when compared to any SAC/substrate and eutectic Sn-Pb/substrate used in the present investigation.

Acknowledgment

Authors thank the Defence Research Development Organization (DRDO) for funding this work under a R&D project grant.

References

1. M. Matahir, L.T. Chin, K.S. Tan, and A.O. Olofinjana, Mechanical Strength and Its Variability in Bi-Modified Sn-Ag-Cu Solder Alloy, *J. Achiev. Mater. Manuf. Eng.*, 2011, **46**, p 50–56
2. S.D. Rani and G.S. Murthy, Evaluation of Bulk Mechanical Properties of Selected Lead-Free Solders in Tension and in Shear, *J. Mater. Eng. Perform.*, 2013, **22**, p 2359–2365
3. M.A. Dudek, R.S. Sidhu, and N. Chawla, Novel Rare-Earth-Containing Lead-Free Solders with Enhanced Ductility, *J. Miner. Met. Mater. Soc.*, 2006, **58**, p 57–66
4. R. Darveaux and C. Reichman, Mechanical Properties Of Lead Free Solders, in *Proceedings of the Electronic Components and Technology Conference*, USA, May 29-1 June 2007, p. 695–706
5. M.G. Affendy and A.A. Mohamad, Effects of Crosshead Speeds on Solder Strength of Cu/Sn–9Zn/Cu Lap Joints, *J. King Saud Univ. Sci.*, 2015, **27**, p 225–231
6. X.F. Wei, Y.K. Zhang, R.C. Wang, and Y. Feng, Microstructural Evolution and Shear Strength of AuSn20/Ni Single Lap Solder Joints, *Microelectron. Reliab.*, 2013, **53**, p 748–754
7. Y.H. Lee and H.T. Lee, Shear Strength And Interfacial Microstructure of Sn-Ag-*x*Ni/Cu Single Shear Lap Solder Joints, *Mater. Sci. Eng. A*, 2007, **444**, p 75–83
8. J.H.L. Pang and B.S. Xiong, Mechanical Properties for 95.5Sn-3.8Ag-0.7Cu Lead-Free Solder Alloy, *IEEE Trans. Compon. Packag. Technol.*, 2005, **28**, p 830–840
9. S.W. Jeong, J.H. Kim, and H.M. Lee, Effect of Cooling Rate on Growth of the Intermetallic Compound and Fracture Mode of Near-Eutectic Sn-Ag-Cu/Cu Pad: Before and After Aging, *J. Electron. Mater.*, 2004, **33**, p 1530–1544
10. M. Sona and K.N. Prabhu, Effect of Reflow Time on Wetting Behavior, Microstructure Evolution, and Joint Strength of Sn-2.5Ag-0.5Cu Solder on Bare and Nickel-Coated Copper Substrates, *J. Electron. Mater.*, 2016, **45**, p 3744–3758
11. M. Sona and K.N. Prabhu, Effect of Reflow Time on Wetting Behaviour, Interfacial Reaction and Shear Strength of Sn-0.3Ag-0.7Cu Solder/Cu Joint, *SMTA J.*, 2015, **28**, p 36–41
12. Satyanarayan and K.N. Prabhu, Reactive Wetting, Evolution of Interfacial and Bulk IMCs and Their Effect on Mechanical Properties of Eutectic Sn-Cu Solder Alloy, *Adv. Colloids Interface Sci.*, 2011, **166**, p 87–188
13. K.J. Lau, C.Y. Tang, P.C. Tse, C.L. Chow, S.P. Ng, C.P. Tsui, and B. Rao, Microscopic Experimental Investigation on Shear Failure of Solder Joints, *Int. J. Fract.*, 2004, **130**, p 617–634
14. J.A. Wasynczuk and G.K Lucey, Shear Creep of Cu_6Sn_5/Sn-Pb Eutectic Composites, in *Proceedings of the Technical Program*, the *National Electronic Packaging and Production Conference*, CA, 1992, pp. 1245–1255
15. R.B. Clough, A.J. Shapiro, A.J. Bayba, and G.K. Lucey, Boundary Layer Fracture in Composite Solder Joints, *Trans. ASME*, 1995, **117**, p 270–274